

Article

Investigation and Numerical Simulation of the Acoustic Target Strength of the Underwater Submarine Vehicle

Kaveripakam Sathish¹, Rajesh Anbazhagan², Ravikumar Chinthaginjala Venkata^{1,*}, Fabio Arena³ 
and Giovanni Pau^{3,*} 

¹ School of Electronics Engineering, Vellore Institute of Technology, Vellore 632014, India

² School of Electrical and Electronics Engineering, SASTRA University, Thanjavur 613401, India

³ Faculty of Engineering and Architecture, Kore University of Enna, 94100 Enna, Italy

* Correspondence: cvrkvit@gmail.com (R.C.V.); giovanni.pau@unikore.it (G.P.)

Abstract: Modern weapon systems' survival hinges on their detection capabilities more than anything else. In the active sonar equation, the acoustic target strength is crucial. Under the assumption of plane wave propagation, the standard target strength equation is used to forecast the reradiated intensity for the far field. The ability of a submarine to remain unnoticed while on patrol or accomplishing a mission is its primary defense. Sonar, sometimes known as sound navigation ranging, is a popular method for locating submarines. This is because saltwater effectively absorbs radio frequencies. Sonar technology is used in more than just the commercial fishing business; it is also used in undersea research. The submarine's designers consider the reflection of acoustic waves to minimize the amount of space required for such reflections. The Target Strength (TS) metric is used to assess the sonar objects' size. This manuscript explains and demystifies the Benchmark Target Echo Strength Simulation (BeTTSi) benchmark submarine's TS analysis. This model's Pressure Acoustic-Boundary Element Model (PA-BEM) interface has been stabilized, and the model itself is pretty huge acoustically.

Keywords: underwater vehicle; target strength; sonar; finite element method; numerical simulation



Citation: Sathish, K.; Anbazhagan, R.; Venkata, R.C.; Arena, F.; Pau, G. Investigation and Numerical Simulation of the Acoustic Target Strength of the Underwater Submarine Vehicle. *Inventions* **2022**, *7*, 111. <https://doi.org/10.3390/inventions7040111>

Academic Editor: Konstantinos G. Arvanitis

Received: 13 November 2022

Accepted: 29 November 2022

Published: 1 December 2022

Publisher's Note: MDPI stays neutral with regard to jurisdictional claims in published maps and institutional affiliations.



Copyright: © 2022 by the authors. Licensee MDPI, Basel, Switzerland. This article is an open access article distributed under the terms and conditions of the Creative Commons Attribution (CC BY) license (<https://creativecommons.org/licenses/by/4.0/>).

1. Introduction

Over the last several decades, acoustic dispersion from submerged objects has been the focus of research and inquiry by many acoustics professionals. Only basic geometrical designs were necessary to provide analytical answers to the issues provided by underwater acoustics [1]. Scientists in the fishing sector used empirical methods, which are approaches based on experience rather than a theory [2]. Furthermore, numerical methods are gaining popularity all the time. In addition to traditional finite element approaches, more complex computational methodologies are being developed to address acoustic issues. For example, the underwater acoustics problem was addressed and solved using the point interpolation approach and the smoothed finite element method [3–7].

However, because the frequency range in which these numerical approaches can be used is limited, they are categorized as middle-frequency techniques. On the other hand, high-frequency techniques include, geometrical acoustics, physical acoustics, and a range of other related areas. Planar elements are based on the Kirchhoff approximation, which demands that a scattering item's dimensions be much greater than the acoustic wavelength [8]. This approximation serves as the basis for the planar element, which is a valuable solution for resolving acoustic difficulties at relatively high frequencies.

Without underwater acoustics, a submarine cannot utilize its stealthy acoustic strategy, as these make detecting and locating a submarine's location feasible. The working frequency of underwater sonar detection equipment has decreased into the lower frequency domain, increasing the stealth performance requirements for submarines, and this is owing to the rapid development of sonar detection technologies for use underwater [9–12]. Determining

the target size allows for a partial evaluation of the stealth effectiveness of a Submarine Target Strength (STS). Researching the Target Strength (TS) of a generic submarine model and analyzing the results revealed that item geometries and structures significantly impact the TS. Because the rudder substantially affects the submarine's TS, it is an essential component of the vessel [13]. The hydrodynamic performance of a rudder is a primary element in its design. When evaluating the capabilities of modern underwater sonar-detecting technology, it is vital to consider the stealth capability of the rudder. Song utilized the Finite Element Method (FEM) to investigate how different materials affect the STS of the rudder. He discovered that the FEM had sufficient precision for relatively low frequencies [14]. In addition, the rudder's shell's thickness and its profile's aspect ratio play significant roles in the rudder's overall structure. Therefore, the design of the rudder can be enhanced by gaining a deeper comprehension of the dynamic relationship between TS and these two factors. These TS-influencing properties of the rudder have never been subjected to a thorough analysis [15–18].

The primary advantage of employing a submarine for military objectives is the crew's ability to remain undiscovered. Submarines were developed in response to the need to lower their optical (visible) footprint considerably. On the other hand, other indicators critical to submarine detection were swiftly discovered. Because of the ease with which sound travels through water, it is possible to detect the presence of submarines using only sound under normal diving conditions.

Passive sonars have been the tool of choice for most detection efforts during the last few decades [19]. They are able to pinpoint the source of the submarine's sonic emissions, and, as a result, tremendous effort was expended to successfully restrict the quantity of radiated acoustic noise created by the submarines. Many navies use active detection sonars because passive sonars have trouble identifying more advanced submarines. Because active sonar detection is critical, the submarine's tendency to reflect incoming acoustic energy Target Echo Strength (TES) must be reduced to a minimum. This is due to the requirement for active sonar detection [20–22].

Not only are procedures for operating submarines constantly updated and improved, but so are the systems for operating sonar. The ever-increasing computing power of computers has dramatically aided sonar technology, resulting in more geometrically exact beams and more complicated data processing procedures [23]. A potential signal-processing method can benefit from the data-synthesis capabilities of a bi- or multi-static network. The fact that this approach has been successfully demonstrated means that the ranges at which a modern submarine may be detected will soon grow dramatically. Submarines must employ TES reduction technologies to maintain their current tactical advantage in the future [24].

Sound transmission in water at distances is characterized by refraction through varying sound speeds with depth (due to temperature, density, and salinity fluctuation) and reflection at water boundaries, as seen in undersea sonar applications.

As a result, sound waves striking a submarine cannot approach from a perfectly horizontal position. More than reducing the TES of a submarine will be required; instead, the TES will need to be dropped across a range of elevation angles. This angular range, also known as the threat sector, is calculated to conduct research on the acoustic propagation of sounds over various sections of the world's oceans. We then compare a standard submarine design to a derivative submarine with a shape optimized for TES [25].

The primary way a submarine defends itself while at work is by maintaining its cover story. Because of the significant amount of radio signal absorbed by seawater, one of the primary methods used for submarine detection is sonar, which stands for sound navigation ranging. While building submarines, engineers consider how acoustic waves are reflected to determine how to minimize the effective area of the sub's reflecting surface. The target strength metric is used to determine the size of a sonar target. Most submarines cover their outside surfaces with absorbent materials to reduce the effect of backscatter signals. Figure 1 depicts the COMSOL Simulation model of the proposed acoustic target strength.

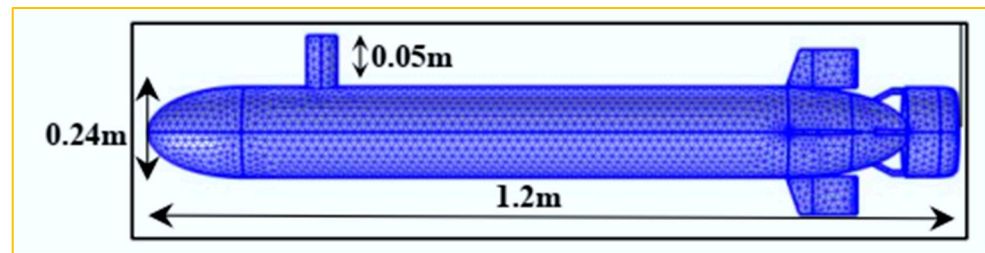


Figure 1. COMSOL Simulation model of proposed acoustic target strength.

The main contribution of the manuscript is highlighted as follows:

- Implementation of acoustic target strength for underwater submarine vehicles;
- Comparison of target strength in different acoustic pressure conditions;
- Analysis of the scattered acoustic sound pressure levels;
- Examination of the radiation pattern in both polar plot and line graph;
- Recommendation of appropriate scattered acoustic sound pressure levels for underwater networks based on the targeted performance metric.

The remaining sections of this work will be structured as follows. In Section 2, we discuss the theoretical definition of a model. In Section 3, we provide the design model and methodology. In Section 4, we provide our findings, comparison, and discussion of the obtained findings, and in Section 5, we conclude the paper.

2. Theoretical Definition of a Proposed Model

The Background Pressure Field is utilized to simulate a spherical wave approaching the submarine's bow from 1000 m away and at an angle of ϕ equal to 360 degrees. When the waves reach the submarine, they already possess the characteristics of plane waves, which is typical for the region. The ocean attenuation material represents the transmission medium's intrinsic losses throughout the modeling process. The parameters of this attenuation model are derived from a vast amount of experimental data, giving it a semi-analytical quality. In addition to the role performed by depth, temperature, salinity (in the real world), and pH, additional elements, such as viscosity effects in pure water, the relaxing processes of boric acid, and magnesium sulfate, to name a few, also have an effect. Select the Absorption coefficient option within the Impedance border condition to indicate the presence of a soft material placed on one of the hard surfaces. Figure 2 shows the simulation's zoomed-out view of the target's vitality and sweeping angle.

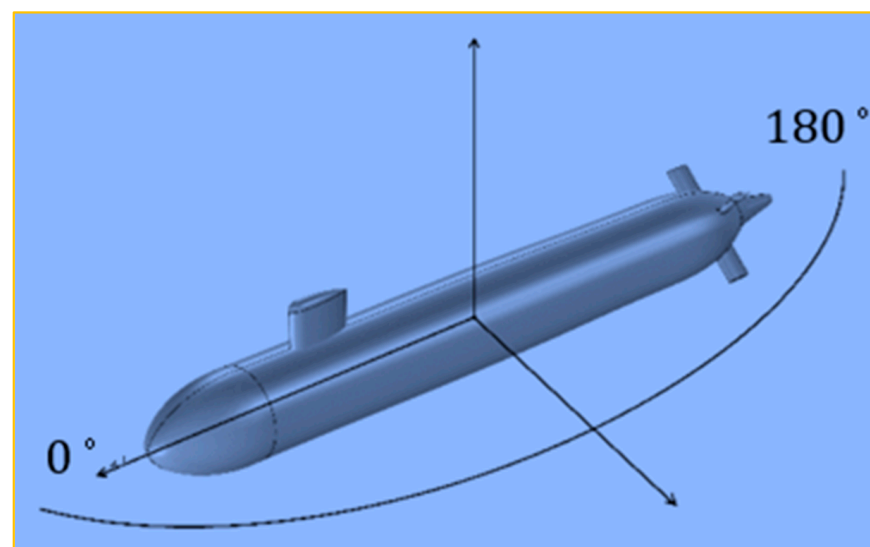


Figure 2. The simulation's zoomed-out view of the target's vitality and its sweeping angle.

During the modelling phase, a boundary element interface is used to build a model:

- In the second stage, we assign geometry and global definitions to the model builder;
- The third step is to configure the pressure acoustics and boundary elements to the model and run simulations of possible model configurations.
- In fourth place, we have a comparison of the results of various valuations of the performance metrics;
- The last stage is collection of the analysis and explanation of the results.

Target strength was calculated using the Helmholtz–Kirchhoff Integral [26,27] and the finite element technique (FEM) for the acoustic–solid coupled model. Target strength is defined by measuring the incident and reflection intensity ratio, and the reference distance is “1 m” in front of the target’s reflection center [28–30].

Simple acoustic fields can be obtained using the wave equation and the Helmholtz equation, but a more complex geometrical model, considering underwater habitats’ boundary conditions, is required to obtain the proper underwater setting [31–33]. This work uses the finite element method (FEM) in conjunction with the governing equation in acoustic–solid connected modules to solve this complicated computation [34–36].

3. Design Model and Methodology

We used COMSOL Multiphysics, version 5.6, in this investigation to simulate the target strength computation. The parameters for performing the simulation are detailed below. Variables evaluated were the target model, vehicle shape, hull thickness, frequency, and sweeping angles of incident acoustic waves. The submarine geometry of BeTSSi is shown in Figure 3.

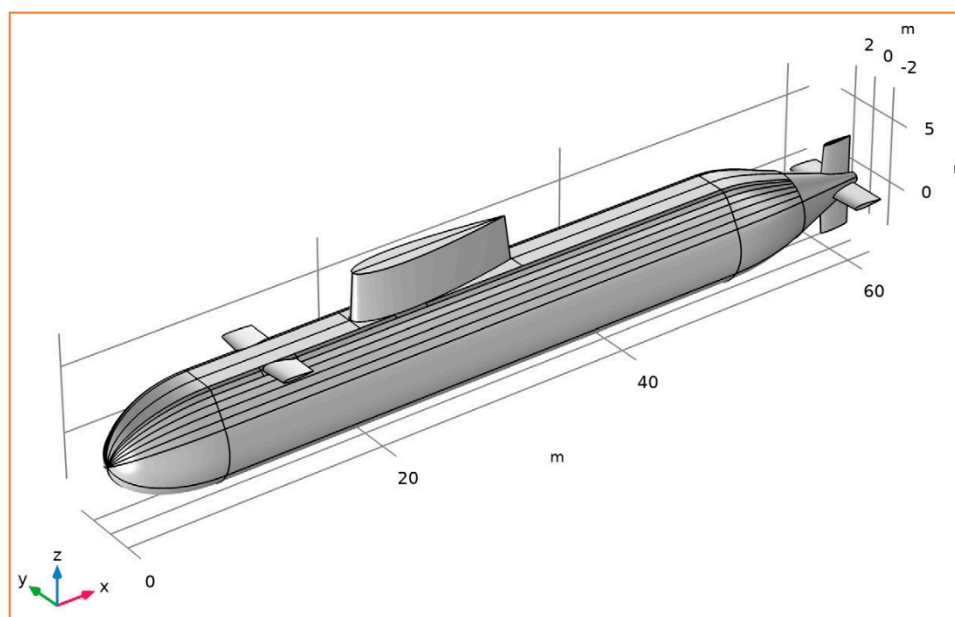


Figure 3. Submarine geometry of BeTSSi.

When measured concerning the wavelength, the dimensions of this model are unacceptably large. Stabilized formulation is used for boundary elements in the physical theory of pressure acoustics. If this way is followed, there is a 100% chance that the iterative solver will converge. When the excitation frequency approaches 800 Hz without remaining stable, iterative solutions call for a significant increase in the number of iterations they perform.

Submarines use an anechoic coating on their hulls to reduce signal scatter. It is possible to make this absorption coefficient dependent on the measurement frequency; in that case, it will use the value specified by the α_n parameter. It is expected that 40 gigabytes of random access memory (RAM) will be required for the analysis, and it will take around

30 min to finish. Because COMSOL relies on virtual memory, the time required to complete a task will lengthen if insufficient RAM is available.

4. Results and Discussion

Target strength (TS) is a critical component in underwater stealth systems. Several studies focus on weakening the target to limit the likelihood of detection. However, the objective strength can be influenced by various factors, including the vehicle's geometries and structures, sonic reflection coefficients, and the material utilized for the outer hull coating, to name a few. We present the results of a calculation of target strength concerning the geometry of the vehicle, the thickness of the hull, and the frequency of acoustic waves incident upon the vehicle in this inquiry. The most challenging component is the demand for enormous amounts of memory and rapid calculation due to the size of the vehicle and the high frequency of the incident acoustic waves. To address this issue, we included a scaling mechanism for the vehicle, which minimizes the model's overall size. In addition, we have increased our computer's capability to improve the accuracy of our calculations. The target strength (TS) is estimated using an acoustic–solid coupled model and the finite element technique (FEM). According to the findings, the personified area and, hence, the TS develops in proportion to the model's size. Greater thickness hulls can be predicted to have a higher TS. Finally, the frequency would impact TS due to the activation of individual auditory modes.

Figure 4 illustrates the total acoustic pressure at the underwater surface areas. Take note of the virtually flat pressure waves and the fact that the “dark” side of the source has far lower acoustic pressure. This is a highly comprehensive acoustical model, as seen by the staggering amount of wavelengths that have been considered.

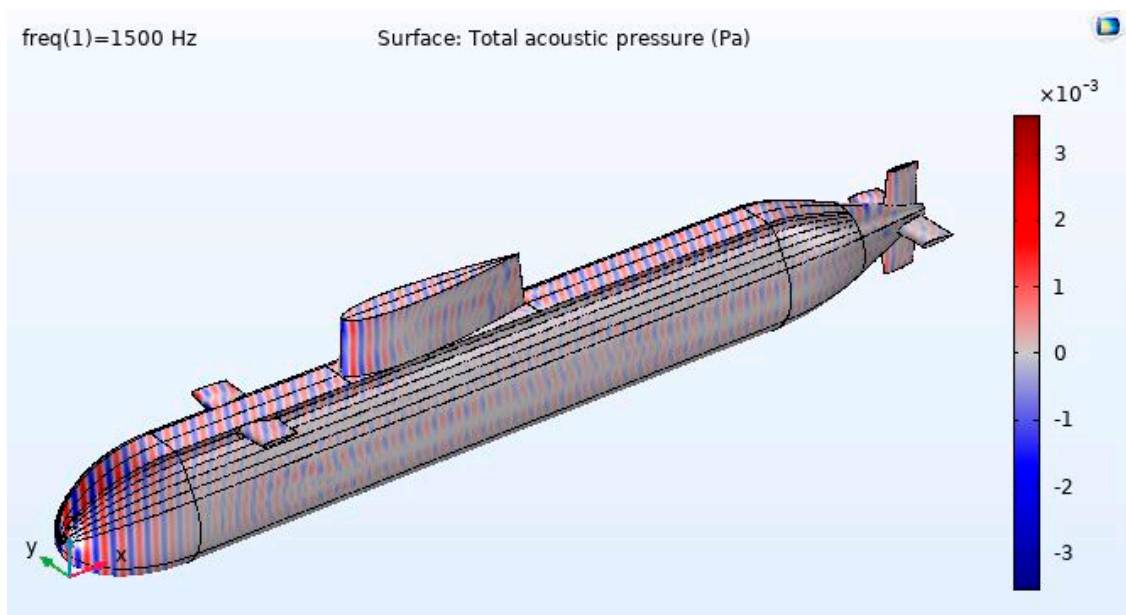


Figure 4. The total acoustic pressure that was measured at the submarine.

Figure 5 illustrates the radiation pattern that would be observed at a distance of one hundred meters from the submarine. To illustrate this, an arrow has been drawn in the general direction that the sound will move. It is important to note that the scattered signal at this frequency has intricate lobes and is extremely position-dependent.

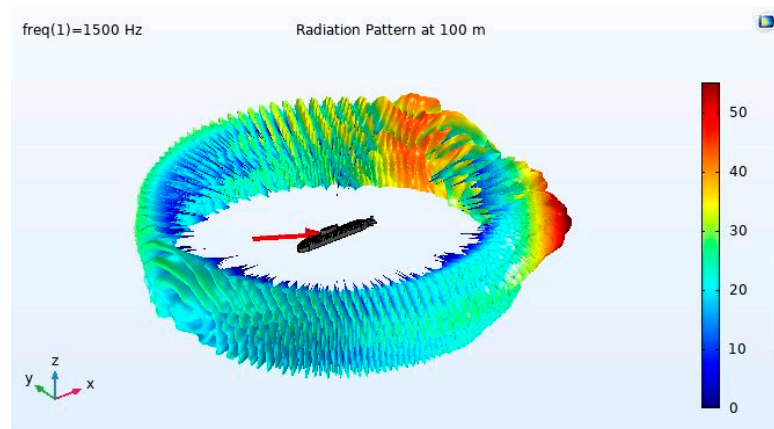


Figure 5. The pattern of radiation one hundred meters distant from the submarine.

Figure 6 shows a cross-sectional image of distributed acoustic pressure through the midsection of the submarine. Figure 7 depicts a plot demonstrating the dispersed sound pressure level in the region as another way of presenting the data.

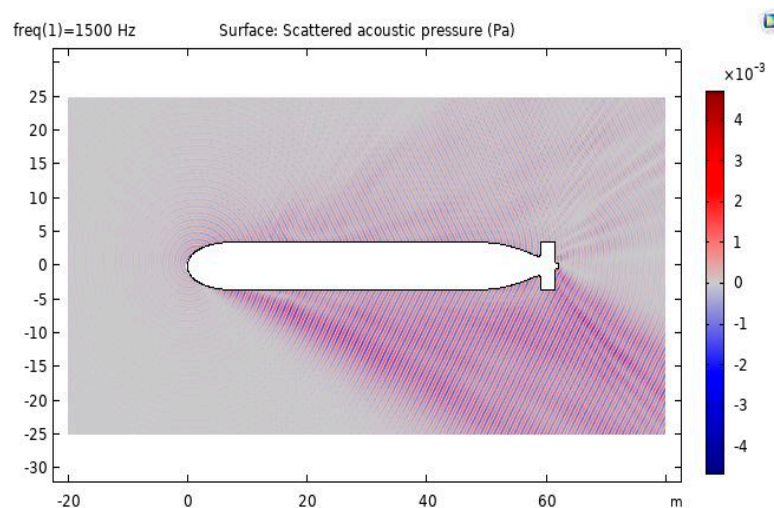


Figure 6. Cross-section of the distributed acoustic pressure.

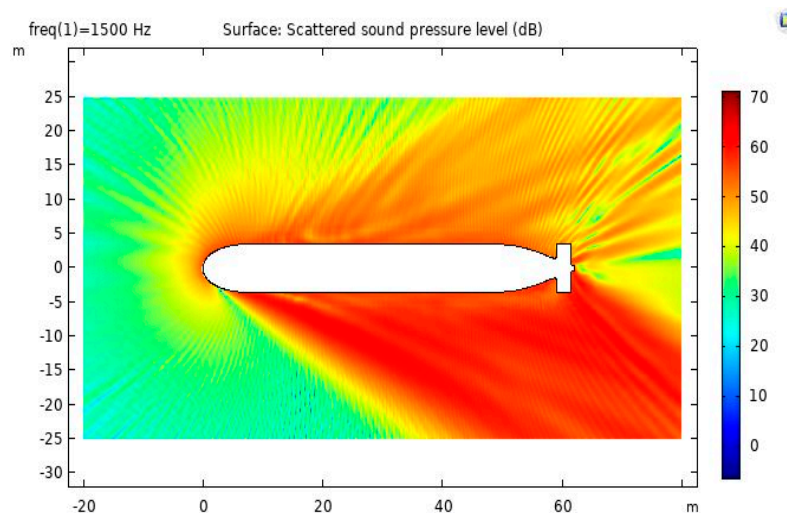


Figure 7. A cross-section at the level of scattered sound pressure.

The target strength (TS) is computed by the following Equation (1):

$$TS = 20 \log_{10} \left[\frac{P_s}{P_{in}} \frac{d_{list}}{1m} \right] \quad (1)$$

where P_s is the scattered pressure at the listening point, P_{in} is the background pressure at the submarine and d_{list} is the distance from the submarine to the listening point. We have used d_source in the simulation of the COMSOL tool as the distance to the listening point, and this equation has been modified in the variable definition.

Figure 7 shows the sound pressure level polar plot around the submarine; that is, the radiation pattern. Note the peaks right below the submarine and at the reflection angle from the source. Sound pressure levels and the resulting radiation pattern surrounding the submarine are seen in Figure 8 below. Take heed of the peaks directly below the submarine and at the reflection angle from the source. Sonar equipment can operate in either an active or passive mode. The distinction between active and passive sonar is that active sonar employs an active source to generate an acoustic signal that is subsequently reflected on the submarine. In contrast, passive sonar includes the sensor reflecting the sound emitted by the submarine while it operates. Active sonar can be utilized in monostatic (source and listening point in the exact location) and bistatic (source and listening point in distinct locations) configurations in the COMSOL acoustic simulation model. The goal strength for a bistatic system is represented in Figure 9.

Radiation Pattern: Scattered sound pressure level (dB)

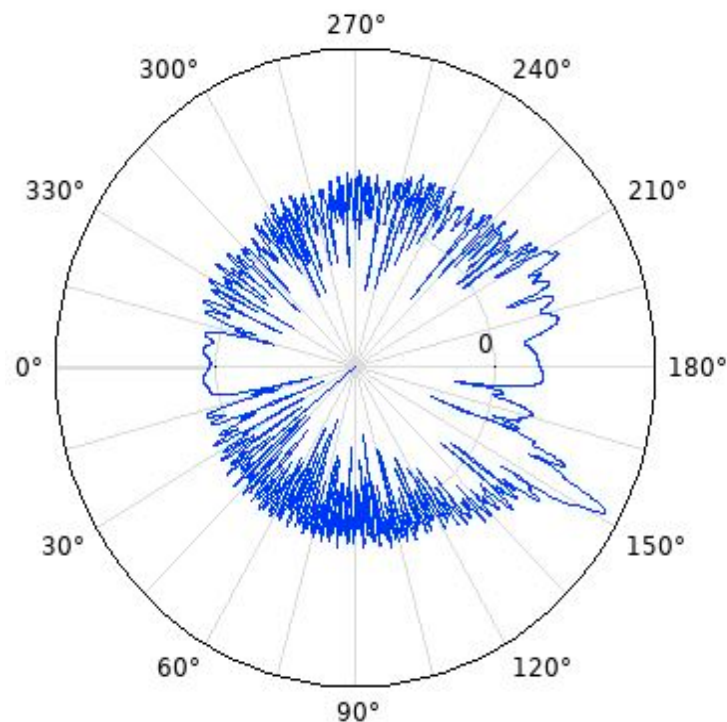


Figure 8. The polar plot of the sound pressure.

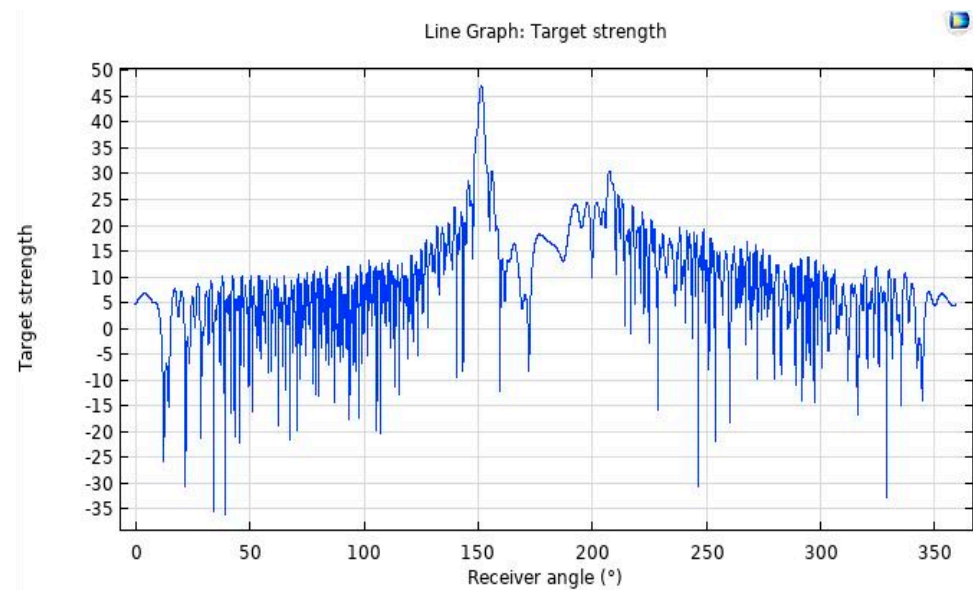


Figure 9. The static target strength of the submarine from a bistatic perspective for a receiver that is located at the same distance as the source.

5. Conclusions

We compared the target strength over three different vehicle geometry magnifications, three different hull thicknesses, the standard acoustic impedance, and a variety of incident acoustic wave frequencies and sweeping angles as part of this research. We also examined the frequency and angle of arrival of the sound waves. To represent the findings of the far-field computation, which relied on the Hamz–Kisshoff integral theory, we used COMSOL Multiphysics, a finite-element analysis program. According to the findings, altering the characteristic acoustic impedance was a critical component of stealth technology. The intensity of the target can be substantially reduced by adding the coating. If the undersea vehicle is more prominent in size, more force will be applied to the target. If the sonar system works at a higher frequency, it is more likely to be noticed. As a result, the anti-high-frequency shielding will be incorporated into the ship’s design for the underwater vehicle.

Author Contributions: K.S.: Conceptualization, Data curation, Formal Analysis, Methodology, Software, Writing—original draft; R.A.: Visualization, Investigation, Formal Analysis, Software; R.C.V.: Supervision, Writing—review & editing, Project administration, Visualization; F.A.: Supervision, Project administration, Visualization; G.P.: Data Curation, Investigation, Resources, Software, Writing—original draft, Methodology. All authors have read and agreed to the published version of the manuscript.

Funding: This research received no external funding.

Institutional Review Board Statement: Not applicable.

Informed Consent Statement: Not applicable.

Data Availability Statement: Data will be made available on request.

Conflicts of Interest: The authors declare no conflict of interest.

References

1. Zampolli, M.; Tesei, A.; Jensen, F.B.; Malm, N.; Blottman, J.B. A computationally efficient finite element model with perfectly matched layers applied to scattering from axially symmetric objects. *J. Acoust. Soc. Am.* **2007**, *122*, 1472–1485. [[CrossRef](#)]
2. Sathish, K.; Ravikumar, C.V.; Srinivasulu, A.; Rajesh, A.; Oyerinde, O.O. Performance and Improvement Analysis of the Underwater WSN Using a Diverse Routing Protocol Approach. *J. Comput. Netw. Commun.* **2022**, *2022*, 9418392. [[CrossRef](#)]
3. Fang, Z.; Hu, W.; Zhang, W.; Chen, S. Kernel correlation filtering multi-object tracking algorithm based on background difference method. *Electron. Meas. Technol.* **2018**, *41*, 68–72.

4. Erol, M.; Vieira, L.F.M.; Caruso, A.; Paparella, F.; Gerla, M.; Oktug, S. Multi Stage Underwater Sensor Localization Using Mobile Beacons. In Proceedings of the 2008 Second International Conference on Sensor Technologies and Applications, Washington, DC, USA, 25–31 August 2008; pp. 710–714. [[CrossRef](#)]
5. Heidemann, J.; Ye, W.; Wills, J.; Syed, A.; Li, Y. Research challenges and applications for underwater sensor networking. In Proceedings of the IEEE Wireless Communications and Networking Conference (WCNC 2006), Las Vegas, NV, USA, 3–6 April 2006; Volume 1, pp. 228–235. [[CrossRef](#)]
6. Sathish, K.; Ravikumar, C.V.; Rajesh, A.; Pau, G. Underwater Wireless Sensor Network Performance Analysis Using Diverse Routing Protocols. *J. Sens. Actuator Netw.* **2022**, *11*, 64. [[CrossRef](#)]
7. Cui, J.H.; Kong, J.; Gerla, M.; Zhou, S. The challenges of building mobile underwater wireless networks for aquatic applications. *IEEE Netw.* **2006**, *20*, 12–18.
8. Wang, K.; Gao, H.; Xu, X.; Jiang, J.; Yue, D. An Energy-Efficient Reliable Data Transmission Scheme for Complex Environmental Monitoring in Underwater Acoustic Sensor Networks. *IEEE Sens. J.* **2015**, *16*, 4051–4062. [[CrossRef](#)]
9. Awan, K.M.; Shah, P.A.; Iqbal, K.; Gillani, S.; Ahmad, W.; Nam, Y. Underwater Wireless Sensor Networks: A Review of Recent Issues and Challenges. *Wirel. Commun. Mob. Comput.* **2019**, *2019*, 6470359. [[CrossRef](#)]
10. Han, G.; Jiang, J.; Shu, L.; Xu, Y.; Wang, F. Localization Algorithms of Underwater Wireless Sensor Networks: A Survey. *Sensors* **2012**, *12*, 2026–2061. [[CrossRef](#)]
11. Sathish, K.; Ravikumar, C.V.; Srinivasulu, A.; Gupta, A.K. Performance Analysis of Underwater Wireless Sensor Network by Deploying FTP, CBR, and VBR as Applications. *J. Comput. Netw. Commun.* **2022**, *2022*, 1–30. [[CrossRef](#)]
12. Yuan, F.; Zhan, Y.; Wang, Y. Data Density Correlation Degree Clustering Method for Data Aggregation in WSN. *IEEE Sens. J.* **2013**, *14*, 1089–1098. [[CrossRef](#)]
13. Agarwal, R.; Kumar, S.; Hegde, R.M. Algorithms for Crowd Surveillance Using Passive Acoustic Sensors over a Multimodal Sensor Network. *IEEE Sens. J.* **2014**, *15*, 1920–1930. [[CrossRef](#)]
14. Teja, G.S.; Samundiswary, P. Performance analysis of DYMO protocol for IEEE 802.15. 4 based WSNs with mobile nodes. In Proceedings of the Computer Communication and Informatics (ICCCI), Coimbatore, India, 3–5 January 2014; pp. 1–5.
15. Ravikumar, C.V.; Kala Praveen, B. Detection of Signals in MC-CDMA Using a Novel Iterative Block Decision Feedback Equalizer. *IEEE Access* **2022**, *10*, 105674–105684. [[CrossRef](#)]
16. Domingo, M.C.; Prior, R. Energy analysis of routing protocols for underwater wireless sensor networks. *Comput. Commun.* **2008**, *31*, 1227–1238. [[CrossRef](#)]
17. Patil, M.S.A.; Mishra, M.P. Improved mobicast routing protocol to minimize energy consumption for underwater wireless sensor networks. *Int. J. Res. Sci. Eng.* **2017**, *3*, 197–204.
18. Manjula, S.H.; Abhilash, C.N.; Shaila, K.; Venugopal, K.R.; Patnaik, L.M. Performance of AODV routing protocol using group and entity mobility models in wireless sensor networks. In Proceedings of the International MultiConference of Engineers and Computer Scientist (IMECS 2008), Hong Kong, China, 19–21 March 2008; Volume 2, pp. 1212–1217.
19. Xiao, X.; Huang, H.; Wang, W. Underwater Wireless Sensor Networks: An Energy-Efficient Clustering Routing Protocol Based on Data Fusion and Genetic Algorithms. *Appl. Sci.* **2021**, *11*, 312. [[CrossRef](#)]
20. Bhattacharjya, K.; Alam, S.; De, D. CUWSN: Energy efficient routing protocol selection for cluster based underwater wireless sensor network. *Microsyst. Technol.* **2019**, *28*, 543–559. [[CrossRef](#)]
21. Mohan, P.; Subramani, N.; Alotaibi, Y.; Alghamdi, S.; Khalaf, O.I.; Ulaganathan, S. Improved Metaheuristics-Based Clustering with Multihop Routing Protocol for Underwater Wireless Sensor Networks. *Sensors* **2022**, *22*, 1618. [[CrossRef](#)]
22. Alkindi, Z.; Alzeidi, N.; Touzene, B.A.A. Performance evolution of grid based routing protocol for underwater wireless sensor networks under different mobile models. *Int. J. Wirel. Mob. Netw.* **2018**, *10*, 13–25.
23. Han, L.; Li, Z.; Liu, W.; Qu, W.; Nie, L.; Zheng, L.; Liu, M. Sensor localization in underwater sensor networks using distance transform-based skeleton extraction. In Proceedings of the 2016 2nd IEEE International Conference on Computer and Communications (ICCC), Chengdu, China, 14–17 October 2016; pp. 2223–2226. [[CrossRef](#)]
24. Peng, R.; Sichitiu, M.L. Angle of arrival localization for wireless sensor networks. In Proceedings of the 2006 3rd Annual IEEE Communications Society on Sensor and Ad Hoc Communications and Networks, Reston, VA, USA, 25–28 September 2006; pp. 374–382.
25. Zhou, Y.; Chen, K.; He, J.; Chen, J.; Liang, A. A Hierarchical Localization Scheme for Large Scale Underwater Wireless Sensor Networks. In Proceedings of the 2009 11th IEEE International Conference on High Performance Computing and Communications, Seoul, Republic of Korea, 25–27 June 2009; pp. 470–475. [[CrossRef](#)]
26. Ullah, I.; Ming-Sheng, G.A.O.; Kamal, M.M.; Khan, Z. A survey on an underwater localization, localization techniques and its algorithms. In *3rd Annual International Conference on Electronics, Electrical Engineering and Information Science (EEEIS 2017)*; Atlantis Press: Dordrecht, The Netherlands, 2017; pp. 252–259.
27. Zarar, S.; Javaid, N.; Zaki, S.M.; Ejaz, M.; Khan, Z.A.; Qasim, U.; Hussain, S. Increased throughput db-ebh protocol in underwater wireless sensor networks. In Proceedings of the 2016 30th International Conference on Advanced Information Networking and Applications Workshops (WAINA), Crans-Montana, Switzerland, 23–25 March 2016; pp. 571–576.
28. Beniwal, M.; Singh, R. Localization techniques and their challenges in underwater wireless sensor networks. *Int. J. Comput. Sci. Inf. Technol.* **2014**, *5*, 4706–4710.

29. Thulasiraman, P.; White, K.A. Topology control of tactical wireless sensor networks using energy efficient zone routing. *Digit. Commun. Netw.* **2016**, *2*, 1–14. [[CrossRef](#)]
30. Pughat, A.; Sharma, V. Performance analysis of an improved dynamic power management model in wireless sensor node. *Digit. Commun. Netw.* **2017**, *3*, 19–29. [[CrossRef](#)]
31. Qasim, M.; Khan, M.; Mehmood, W.; Sobieczky, F.; Pichler, M.; Moser, B. A Comparative Analysis of Anomaly Detection Methods for Predictive Maintenance in SME. In *International Conference on Database and Expert Systems Applications*; Springer: Cham, Switzerland, 2022; pp. 22–31. [[CrossRef](#)]
32. Khan, M.; Ahmad, A.; Sobieczky, F.; Pichler, M.; Moser, B.A.; Bukovsky, I. A Systematic Mapping Study of Predictive Maintenance in SMEs. *IEEE Access* **2022**, *10*, 88738–88749. [[CrossRef](#)]
33. Khan, M.; Liu, M.; Dou, W.; Yu, S. vGraph: Graph Virtualization towards Big Data. In *Proceedings of the 2015 Third International Conference on Advanced Cloud and Big Data*, Yangzhou, China, 30 October–1 November 2015; pp. 153–158. [[CrossRef](#)]
34. Rafique, W.; Khan, M.; Sarwar, N.; Sohail, M.; Irshad, A. A Graph Theory Based Method to Extract Social Structure in the Society. In *International Conference on Intelligent Technologies and Applications*; Springer: Singapore, 2019; pp. 437–448. [[CrossRef](#)]
35. Haindl, P.; Buchgeher, G.; Khan, M.; Moser, B. Towards a reference software architecture for human-AI teaming in smart manufacturing. *arXiv* **2022**, arXiv:2201.04876. [[CrossRef](#)]
36. Cv, R.; Sathish, K. Performance Analysis of Clustered Based Underwater Wireless Sensor Network by Deploying Application as CBR. In *Proceedings of the 2022 Third International Conference on Intelligent Computing Instrumentation and Control Technologies (ICICICT)*, Kannur, India, 11–12 August 2022; pp. 1678–1686. [[CrossRef](#)]